https://doi.org/10.1590/S1413-415220220230

Scientific Paper

Mining waste acting as a precursor of environmental stress in sediments

Rejeitos de mineração atuando como precursores de estresse ambiental em sedimentos

Paulo Roberto Bairros da Silva[1], Denise Parizotto[2], Leonardo Roggen e Silva[2], Paulo Sergio Parreira[3], Fabio Luiz Melquiades[3], Frederico Fábio Mauad[2]

ABSTRACT

Waste generated by mineral extraction is globally associated with environmental disturbances due to its deleterious effect on water resources. However, research focused on the influence of mine tailings resulting from the extraction of semi-precious stones on fluvial systems is still incipient in the environmental literature. From this perspective, this study quantified the average concentrations of major oxides present in the fine fractions of the sediment samples from the Várzea river, in the State of Rio Grande do Sul, southern Brazil, using wavelength dispersive X-ray fluorescence spectrometry. This region is acknowledged as the largest rock amethyst mining area in the world. Additionally, geochemical indices were established to characterize potential sources of production, maturity, degree of weathering, and sediment pollution. To evaluate the influence of mine tailings on the Várzea river sediments, the contents of Al_2O_3, Fe_2O_3, MnO, P_2O_5, CaO, SiO_2, K_2O, CuO, ZnO, and TiO_2 major oxides present in sediment samples were determined and compared to the local background values; the values varied significantly ($p < 0.05$), classifying them as polluted and medium polluted. Also, the sediment samples with evident characteristics of extreme chemical weathering consist mainly of clay minerals and mafic igneous rocks, and similarities were found between sediment samples and tailings from the mineral extraction zone. The Principal Component Analysis and the cluster analysis also suggest the existence of three distinct mineral oxide groups, differentiating the zones leaving and upstream the mining zone from the other sampling points.

Keywords: mineral prospecting; Ametista do Sul; geochemistry; WD-XRF.

RESUMO

Os rejeitos de atividades de extração mineral são mundialmente associados a distúrbios ambientais devido a sua capacidade de atuação deletéria sobre os recursos hídricos. No entanto, o número de estudos sobre a influência dos rejeitos de zonas de extração de rochas semipreciosas sobre sistemas flúvicos ainda é incipiente na literatura da área ambiental. Nessa perspectiva, foram quantificadas pela técnica de espectrometria de fluorescência de raios-X por dispersão de comprimento de onda as concentrações médias de óxidos minerais majoritários presentes nas frações finas das amostras de sedimentos do Rio da Várzea, Sul do Brasil, maior região mundial extratora de rochas ametista. Somado a isso, avaliou-se a qualidade ambiental e caracterizaram-se as potenciais fontes por meio de índices geoquímicos. Os resultados consideram a provável influência dos rejeitos de mineração sobre os sedimentos do rio da Várzea, classificando-os como não poluído a moderadamente poluído e, quando comparados ao *background* local, apresentam variâncias significativas ($p < 0{,}05$) para os óxidos minerais Al_2O_3, MnO, CaO, SiO_2, K_2O e TiO_2. Além disso, as amostras de sedimentos que apresentaram características de intemperismo químico extremo são formadas por argilominerais e rochas ígneas máficas, e foram encontradas similaridades entre as amostras de sedimentos e os rejeitos da zona de extração mineral. Conclui-se que os rejeitos de rochas basálticas, acúmulos de fronte aos garimpos, funcionam como fonte de estresse ambiental no sistema hídrico.

Palavras-chave: prospecção mineral; Ametista do Sul; geoquímica; WD-XRF.

INTRODUCTION

Mineral extraction activities affect the environmental quality of adjacent water systems, causing deleterious changes to ecosystems (BECK *et al.*, 2020; GLOAGUEN; MOTTA; COUTO, 2021; KUSIN *et al.*, 2019; SILVA *et al.*, 2019). In these activities, the environmental contamination results from the rainwater ability to fractionate, solubilize and transport minerals and inorganic compounds (metals, semimetals, and non-metals) found in the tailings from mining (AMOSOVA *et al.*, 2019; BESSA *et al.*, 2020; GUILHEN *et al.*, 2019; SILVA *et al.*, 2019).

[1]Universidade Federal de Santa Maria, Departamento de Geociências – Santa Maria (RS), Brazil.
[2]Universidade de São Paulo, Escola de Engenharia de São Carlos – São Carlos (SP), Brazil.
[3]Universidade Estadual de Londrina (UEL), Departamento de Física – Londrina (PR), Brazil.
***Corresponding author:** paulo.bairros-silva@ufsm.br
Conflicts of interest: the authors declare no conflicts of interest.
Funding: none.
Received on: 08/31/2022 – **Accepted on:** 11/18/2022

Mine tailings are associated with environmental disturbances, such as acid mine drainage, reduced hydrogen and redox potential, restricted oxygen concentrations, elevated salinization, and changed alkalinity due to reactions with carbonates while also favoring sediment production/loading (SANG *et al.*, 2018; SILVA *et al.*, 2019; ZHAO *et al.*, 2020). Mine tailings carried into the aquatic environment, via surface processes (adsorption, complexation, and reprecipitation), tend to decant and become part of the fluvic sediments (BECK *et al.*, 2020; REMOR *et al.*, 2018; SUNDARARAJAN *et al.*, 2017). In Brazil, the contamination that occurred in recent years in Brumadinho, Mariana, and Santo Antônio do Grama (cities in the state of Minas Gerais) and Barcarena (city in the state of Pará) due to mine tailings demonstrate the difficulty of addressing this environmental problem (ALVES; FERREIRA; ARAÚJO, 2021; PASTRAN; MALLETT 2020; SILVA *et al.*, 2019).

Sediments are complex, multi-element and polygranular environmental matrices, whose ability to store and diffuse inorganic compounds turn them into environmental stressors that can directly interfere with the aquatic ecosystem dynamics (HERATH *et al.*, 2018; SILVA *et al.*, 2016; SILVA *et al.*, 2019). The term 'environmental stressor' describes chemical elements, biological or physical entities in sediments that may cause adverse effects (BURTON; JOHNSTON, 2010; SILVA *et al.*, 2016; USEPA, 1992).

Nevertheless, sediments are also an essential, integral, and dynamic part of water systems, such as rivers and lakes, while human activities, such as mineral extraction, directly affect sediment quantity and composition, making environmental planning and management actions necessary (LONE *et al.*, 2018; MIZAEL *et al.*, 2020; SILVA *et al.*, 2016). In watersheds with mining activities, the concentrations of certain chemical compounds can indicate tailings influence as a residue/waste source, contributing to the water system and interfering in the environmental quality (GOMES; ALMEIDA; SPERANDIO, 2018; KUSIN *et al.*, 2019; SILVA *et al.*, 2019).

Understanding the mobility of major oxides during the weathering processes has been proposed as an alternative to identify sediment formation zones (GOMES; ALMEIDA; SPERANDIO, 2018; SANG *et al.*, 2018; SILVA *et al.*, 2019; SOUSA *et al.*, 2018). Additionally, sediment quality is often assessed by environmental geochemical indices based on average concentrations of local inorganic chemical compounds, the background values, compared to bottom levels as a tool for water resource management (BILLAH; KOKUSHI; UNO, 2019; MIZAEL *et al.*, 2020).

This method considers that variations of the average concentrations of fluvial sediments are associated with adverse effects on aquatic ecosystems, allowing to track down where such environmental stress sources are located (HERATH *et al.*, 2018; KUSIN *et al.*, 2019; SUNDARARAJAN *et al.*, 2017). For this purpose, this study uses this approach in the semi-precious rock extraction zones to assess the influence of mine tailings on local water systems since there are few studies in the literature applying this methodology (DIAS *et al.*, 2019; HARTMANN; PERTILLE; DUARTE, 2017; SILVA *et al.*, 2019). Besides, geochemical concentrations in sediments were characterized and quantified to determine the potential influence of mining tailings, the respective sources, and to assess the quality of sediments by determining the geochemical indices, on the Várzea river, a water system located in southern Brazil, the region with the largest amethyst extraction in the world (DIAS *et al.*, 2019; SILVA *et al.*, 2019; VOSOOGH; SAEEDI; LAK, 2016).

Although Silva *et al.* (2019) investigated sediment contamination in the mining region of the Várzea river, using an energy dispersive X-ray fluorescence spectrometer (EDXRF — Shimadzu equipment, model EDX-720, Rannye Series), and established environmental quality indices, these authors did not address the geochemical characterization through indices based on the mean concentrations of the major mineral oxides that structure sediment samples. This gap is intended to be filled in this upcoming study, through instrumental analyzes performed with a wavelength dispersive X-ray fluorescence spectrometer (WDXRF — BRUKER, model S8 TIGER), allowing to determine the condition of weathering and identifying its source and main characteristics.

MATERIAL AND METHODS

Study site

Located in the northern region of Rio Grande do Sul (Southern Brazil), the Várzea river length is approximately 165 km and it drains an area of 9,324 km^2 (Figure 1). It is one of the main left-bank tributaries of the Uruguay river, in the hydrographic region of Uruguay (FEPAM, 2020; SEMA, 2012; SILVA *et al.*, 2019).

The Várzea river flows through regions with a dense red dystrophic red latosol soil, characterized by strong acidity and low nutrient reserve that usually requires fertility corrections. The main agricultural activities are crops

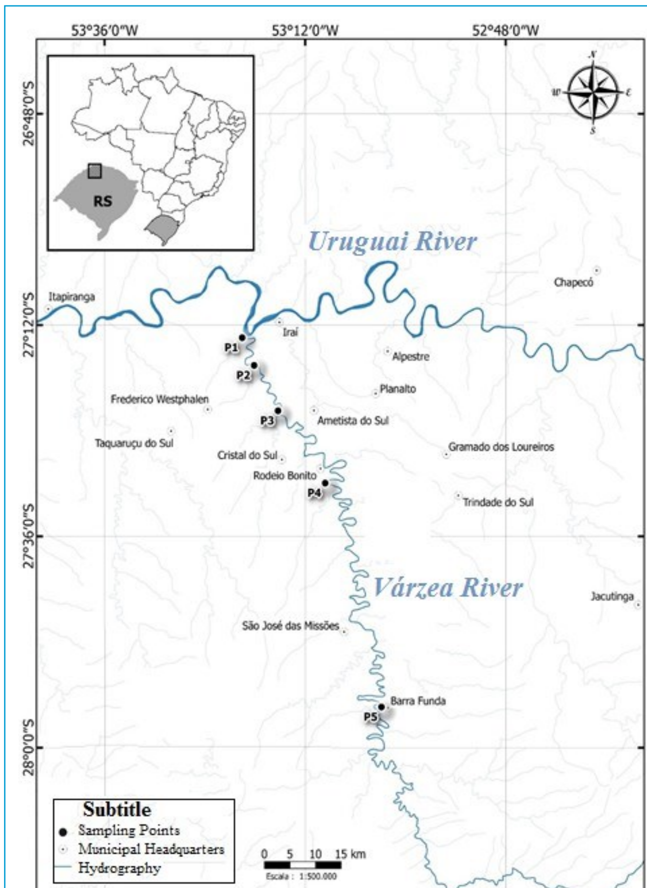

Source: elaborated by the authors.

Figure 1 – Hydrographic map containing the spatial and fluvial distribution of the Várzea river showing the sediment sampling points.

(wheat, corn, and soybeans) and animal husbandry (chicken, pork, and cattle) (SANTOS *et al.*, 2018; MSRS, 2020). In the northern portion of the Várzea river, semi-precious rocks (amethyst, quartz, agate, and calcite) are mined in horizontal underground mines. Figure 1 shows the municipalities of Ametista do Sul, the world's largest producer of amethyst, as well as Frederico Westphalen, Rodeio Bonito, Cristal do Sul, Planalto, Iraí, Trindade do Sul, and Gramado dos Loureiros (HARTMANN; PERTILLE; DUARTE, 2017; KORCHAGIN; CANER; BORTOLUZZI, 2019).

The genesis of the semi-precious rocks is attributed to volcanic deposits in the Paraná basin from the basaltic flows related to the Serra Geral formation, resulting from the interaction of hydrothermal events associated with the Guarani aquifer (BAGGIO *et al.*, 2015; DIAS *et al.*, 2019; KORCHAGIN; CANER; BORTOLUZZI, 2019). Figure 2 showed the semi-precious rocks extracted in the region.

Several studies characterize the concentrations of elements present in the basalt residues to determine the formation and geochemical extent of the semi-precious rocks (HARTMANN *et al.*, 2015; KORCHAGIN; CANER; BORTOLUZZI, 2019; SILVA *et al.*, 2019). Table 1 shows the average concentration of compounds present in the basalt waste.

However, few studies so far have been able to demonstrate the influence of mineral extraction activities on the quality of sediment in water systems, and also address the influence of this activity as environmental liability generated from tons of tailings from basalt rocks (rocks of volcanic origin rich in iron and magnesium silicates) stored/exposed to weather in front of mines (Figure 3).

Under favorable environmental conditions, these tailings tend to fragment into small particles that end up carried into the Várzea river, possibly leading to harmful environmental effects (BAGGIO *et al.*, 2015; KORCHAGIN; CANER; BORTOLUZZI, 2019; SILVA *et al.*, 2019).

Sediment sampling, storing, and preparation

Figure 1 shows the Várzea river watershed, highlighting the sampling points deemed relevant for this study (upstream, downstream, and inside the mineral extraction zones) regarding both spatial variability and ease of access. The sediment sampling processes followed clean technique protocols, using a stainless-steel Petersen dredge (3 kg) (BRANDÃO *et al.*, 2011; SILVA *et al.*, 2019).

Table 1 – Average concentrations of major oxides present in samples of basalt rock tailings from the mining zone in the northern portion of the Várzea river.

	Baggio *et al.* (2015)	Hartmann *et al.* (2015)	Korchagin; Caner; Bortoluzzi (2019)
	Amethyst: Mina Museum	*Amethyst: Mina Museum*	*Amethyst: Geodes*
	$(\bar{X} \pm CI)$	$(\bar{X} \pm CI)$	$(\bar{X} \pm CI)$
Oxides (%)			
Na_2O	2.36 ± 0.04	2.21 ± 0.03	3.67 ± 0.18
MgO	5.56 ± 0.17	4.41 ± 0.36	5.55 ± 0.36
Al_2O_3	13.08 ± 0.18	14.99 ± 0.54	15.90 ± 0.52
SiO_2	49.42 ± 0.46	46.63 ± 1.28	47.42 ± 1.26
P_2O_5	0.28 ± 0.01	3.58 ± 0.06	0.87 ± 0.02
K_2O	1.13 ± 0.19	1.19 ± 0.23	1.47 ± 0.18
CaO	9.57 ± 0.07	8.10 ± 0.18	8.27 ± 0.28
TiO_2	2.28 ± 0.06	12.21 ± 0.27	3.54 ± 0.17
MnO	0.20 ± 0.02	0.56 ± 0.02	0.20 ± 0.02
Fe_2O_3	14.86 ± 0.61	0.20 ± 0.03	13.85 ± 0.87
ZnO	ND	ND	0.05 ± 0.00
SrO	ND	ND	0.06 ± 0.01

$\bar{X}$: average concentration; CI: confidence interval; ND: non-determined.
Source: reference values for basalt tailings, average concentrations calculated for three rock samples, Baggio *et al.* (2015); 16 samples, Hartmann *et al.* (2015); five samples, Korchagin; Caner; Bortoluzzi (2019).

Source: elaborated by the authors.

Figure 3 – Mine tailings accumulated in front of the mine in Ametista do Sul, Southern Brazil.

Source: elaborated by the authors.

Figure 2 – The semi-precise rocks extracted in the Várzea river mining region (rough rocks and cut jewels), Southern Brazil.

The sampling points in Figure 1 correspond to the municipalities of Iraí, on the BR-386 bridge (at the Iraí and Frederico Westphalen border), downstream from the mining zone (P1); Iraí on the Estrada da Ponte Velha (at the Ametista do Sul and Iraí border), exiting the mining zone (P2); the main mining town of Ametista do Sul (P3); Rodeio Bonito and Cristal do Sul, at the beginning of the mining zone (P4); and Barra Funda, upstream from the mining zone (P5). The sampling dates and geographic location are shown in Table 2.

The sampling protocol consisted of sampling in triple throw, perpendicular to the river cross-section (margins and center), generating composite samples per sampling point that were stored in 2 L polypropylene Ziploc bags, transported in cooling boxes to the laboratory, where they were kept refrigerated in a freezer (-25°C) until the analysis (SILVA *et al.*, 2016; SILVA *et al.*, 2019). For the analysis, the sediment samples were dried in a circulation oven, manually disintegrated using an agate mortar and pestle, and separated into fine fractions (< 0.063 mm) in a sieve shaker system.

Characterizing and quantifying major oxides in sediment samples

The major oxides present in the fine fractions of the sediment samples were characterized using a BRUKER wavelength dispersive X-ray fluorescence spectrometer (WD-XRF), model S8 TIGER (1 KW). The system was equipped for three ranges, the Na and Mg (XS 55 crystal, P10 gas detector), Al to S (PET crystal, P10 gas detector) and above K (LiF200 crystal, scintillation detector), as well as mask in the X-ray tube to irradiate a 28 mm diameter area of the sample. Measurements were performed on powdered sediment samples (4 g, < 63 µm fractions) packed in specific containers covered with 2.5 µm thick mylar film, under He atmosphere, in the Quant Express routine.

The analytical method was calibrated to quantify the major oxides (Al_2O_3, SiO_2, P_2O_5, K_2O, CaO, TiO_2, Fe_2O_3, MgO, MnO, ZnO, and SrO) found in the sediment samples, compared to the certified reference materials (CRM), Mineral Barium Carbonate (IAEA-Co9) of the International Atomic Energy Agency (IAEA); Sediment Green River (SGR-1b) and Sediment Cody (SCo-1) shales, both from the United States Geological Survey (USSG).

The WD-XRF is often used for the geochemical characterization of environmental matrices (sediments, soils, rocks) due to its high precision since the technique does not interfere with the compounds' chemical bonds, besides the low analytical cost compared to other techniques (CROUDACE *et al.*, 2019; GUILHEN *et al.*, 2019; OYEDOTUN, 2018). A total of 45 WD-XRF analyses were performed on the fine fractions of 15 composite sediment samples from the Várzea river, and the results were accepted as consistent according to the level of confidence for environmental matrices (INMETRO, 2018; SILVA *et al.*, 2019).

The quality of the analytical process was linked to the instrumental recovery of major oxides in the CRM (IAEA-Co9, SGR-1b, SCo-1) (Supplementary Figure 1). A good agreement is observed between CRM values and WD-XRF analyses in the laboratory (between 80 and 120%) for Na_2O, MgO, Al_2O_3, SiO_2, P_2O_5, K_2O, CaO, TiO_2, MnO, Fe_2O_3, CuO, ZnO, and SrO.

Statistical analysis and graphs

The outliers were removed by applying the Grubbs test to the datasets of major oxides in the QuickCalcs Outlier Calculator system (DOTMATICS, 2020). The SciDavis software was used for the plots (SOURCEFORGE, 2018), while other data were processed using Microsoft Office softwares. The datasets were submitted to the Jarque-Bera Normality test, Analysis of Variance (ANOVA), and Tukey test using the PAleontological STatistics (PAST) statistical software, Version 3.08 (HAMMER, 2015).

The dendrogram of the Hierarchical Cluster Analysis (Manhattan metric and Ward method) and the Principal Component Analysis (PCA) were performed with a 15 x 13 matrix, referring to 15 samples (sampling points in the sampling campaigns 1, 2, and 3) and 13 variables (each chemical component concentration). The data were self-scaled, and the analyses were performed using the R software (THE R FOUNDATION, [*s.d.*]).

Environmental geochemical indexes

The Chemical Index of Alteration (CIA) determines the degree of chemical weathering of river sediments as it reveals the resistance of aluminum silicates to the formation of clay minerals (GOMES; ALMEIDA; SPERANDIO, 2018; KUSIN *et al.*, 2019; SANG *et al.*, 2018). Equation 1 is used to calculate the CIA scores.

$$CIA = \left(\frac{Al_2O_3}{Al_2O_3 + CaO + Na_2O + K_2O}\right) \times 100 \quad (1)$$

The CIA scores are linked with the concentration of major oxides in the fluvial sediments and allow a better understanding of the sediment formation zones (Table 3).

Also, chemical weathering is usually assessed by equations that establish elementary ratios (ER), as in Equations 2 and 3.

$$ER_1 = \left(\frac{K_2O}{Al_2O_3}\right) \quad (2)$$

$$ER_2 = \left(\frac{Al_2O_3}{TiO_2}\right) \quad (3)$$

Both ER_1 and ER_2 (Table 3) are based on the concentration of major oxides and establish composition indexes that characterize the sediment source rock (GOMES; ALMEIDA; SPERANDIO, 2018; KUSIN *et al.*, 2019; SHEN *et al.*, 2018). The ER_3 and ER_4 ratios, as in Equations 4 and 5, together with the CaO

Table 2 – Sampling campaigns, geographical coordinates of the sampling points of the Várzea river sediments.

Sampling points	Code	Coordinates		Campaigns	Date	Material
Barra Funda	BF	27°55'22" S	53°02'52" W	1°	02/07/2016	Sediments
Rodeio Bonito	RB	27°26'33" S	53°10'13" W	2°	17/09/2016	Sediments
Ametista do Sul	A	27°21'44" S	53°15'16" W			
Iraí – Ponte Velha	IPV	27°16'33" S	53°18'07" W	3°	01/11/2016	Sediments
Iraí – BR-386	IBR	27°13'25" S	53°19'31" W			

Source: elaborated by the authors.

Table 3 – Scores for environmental geochemical indexes.

Value	Chemical Index of Alteration (CIA)	Value	Elementary ratio (ER_1)	Value	Elementary ratio (ER_2)
50 ≤	No chemical weathering	0.0 - 0.3	Clay minerals	3-8	Originated from mafic igneous rocks
50 - 60	Low chemical weathering			8-21	Intermmediate rocks
60 - 80	Moderate chemical weathering	0.3 - 0.9	Feldspars	21-70	Felsic igneous rocks
80 >	Extreme chemical weathering				

Source: elaborated by the authors.

content, have been used to assess the maturity and chemical composition of sediments (SANG *et al*., 2018; ZANARDO *et al*., 2017).

$$ER_3 = \left(\frac{SiO_2}{Al_2O_3}\right) \quad (4)$$

$$ER_4 = \left(\frac{Fe_2O_3}{K_2O}\right) \quad (5)$$

Sediments from different sources have characteristic geochemical signatures (BESSA *et al*., 2020; GLOAGUEN; MOTTA; COUTO, 2021; SHEN *et al*., 2018; SILVA; BATEZELLI; LADEIRA, 2015; SILVA *et al*., 2019). This aspect can be explored to define regions of environmental similarity in diagrams of the K_2O/Na_2O versus SiO_2 type (ARISEKAR *et al*., 2021; SILVA; BATEZELLI; LADEIRA, 2015; ZANARDO *et al*., 2017).

Contamination in sediment samples from the Várzea river was evaluated in relation to the mean concentration of major oxides using the Nemerow Pollution Index (NPI) (ARISEKAR *et al*., 2021; NEMEROW, 1991).

This index considers the mean and maximum values of the Pollution Index (PI) (Equation 6) and highlights chemical species with a high degree of pollution (Equation 7).

$$PI = \frac{C_m}{C_N} \quad (6)$$

$$NPI = \sqrt{\frac{\left(\frac{1}{n}\sum_{i=1}^{n} PI\right)^2 + PI_{max.}^2}{n}} \quad (7)$$

In which:
PI = the calculated single pollution index;
Cm = the metal concentration in the sediment;
Cn = the baseline concentration;
PImax = the maximum value of PI;
n = the number of chemical species considered in the study.

The NPI value is dimensionless and represents the overall pollution provided by a single parameter. As for the degree of pollution, we have that: NPI ≥ 0.5 (sediment no pollution); 0.5 < NPI ≤ 0.7 (sediment clean); 0.7 < NPI ≤ 1.0 (sediment warm); 1.0 < NPI ≤ 2.0 (sediment polluted); 2.0 < NPI ≤ 3.0 (medium pollution); NPI > 3.0 (sediment severe pollution).

RESULTS AND DISCUSSION

Quantifying major oxides in sediment samples

Table 4 shows the average concentrations of major oxides present in the fine fractions (< 63 μm) of the sediment samples measured by WD-XRF.

The statistical results in Table 4 show the variation of the average concentrations of major oxides in the sediment samples considering the spatial variations between the points and the seasonality between the sampling campaigns 1, 2, and 3 (Supplementary Table 1).

The reliability of the results generated with WD-XRF technique (BRUKER, model S8 TIGER) is reinforced by comparing the mean concentrations present in the samples with those presented in the study by Silva *et al.* (2019), who also evaluated the presence of major oxides in sediment samples from the region using the ED-XRF instrumental technique (Shimadzu, model EDX-720).

Table 4 shows that the Na_2O, MnO and SiO_2 concentrations varied significantly between the Barra Funda (upstream the mining zone) sampling point and the others. Also, the MgO and CaO concentrations are significantly different between the Barra Funda (upstream the mining zone) and Rodeio Bonito (beginning of the mining zone) sampling points. Table 4 shows that the P_2O_5 concentration varied significantly between Iraí — BR-386 (IBR) (downstream the mining zone) and the other sampling points.

Statistical analyses of sample datasets

To better explore the WD-XRF analysis results of the fine fractions (< 0.063 mm) of the sediment samples, the sample dataset was subjected to the Grubbs and Jarque-Bera tests (two-tailed, significant $p \geq 0.05$). The results show that the datasets are normally distributed and follow the Gaussian model, thus allowing to use parametric statistics (Supplementary Table 2).

Also, the datasets were submitted to ANOVA to identify significant differences between average sediment samples from different sampling points (upstream and downstream of the mining zone) and sampling campaign (seasonal variation), as shown in Table 5.

The results indicated no significant differences for the Fe_2O_3, CuO, SrO, and ZnO major oxides, but significant for the other analytes. The Tukey test (two-tailed, significant $p \geq 0.05$) results shown in Table 6 identified the major oxides with significant variance in the datasets.

The results also indicate a significant variance of the major oxides Al_2O_3 and TiO_2 between Iraí — Ponte Velha (IPV) (mining zone) and other sampling points. Figure 4 shows the results for the PCA of the sediment samples (Table 4).

In Figure 4, the PCA of the first two components explains 61.7% of the dataset variance. The negative direction of Principal Component (PC) 1 (39.7%) suggests the differentiation of samples with higher levels of MgO, K_2O, SiO_2, CaO, and TiO_2. The third quadrant clusters the IPV sample point (leaving the mining zone) with high ZnO and TiO_2 concentrations.

The fourth quadrant clusters the samples from the Barra Funda (BF) sampling point with higher levels of Fe_2O_3 and CuO. In general, the PCA plots separated the samples into three distinct clusters, the IPV sampling points (leaving the mining zone), other samples, and BF (upstream the mining zone), according

Table 4 – Average concentrations of major oxides in the Várzea river sediment samples.

	ANALYTE	BF		RB		A		IPV		IBR	
		($\overline{X}$ ± CI)	VC (%)	($\overline{X}$ ± CI)	VC (%)	($\overline{X}$ ± CI)	VC (%)	($\overline{X}$ ± CI)	VC (%)	($\overline{X}$ ± CI)	VC (%)
1ª Sampling campaign	Na_2O	0.16 ± 0.01	4.5	0.29 ± 0.01	2.7	0.32 ± 0.01	1.9	0.30 ± 0.01	2.9	0.25 ± 0.06	20.6
	MgO	0.49 ± 0.02	3.3	0.67 ± 0.01	0.3	0.66 ± 0.01	1.3	0.60 ± 0.02	2.9	0.60 ± 0.02	2.9
	Al_2O_3	16.2 ± 0.2	1.3	13.9 ± 0.1	0.9	13.9 ± 0.2	1.3	12.5 ± 0.2	1.4	15.6 ± 0.3	1.5
	SiO_2	41.4 ± 0.6	1.3	44.9 ± 0.2	0.4	43.9 ± 0.3	0.5	44.5 ± 1.1	2.1	43.5 ± 0.5	1.1
	P_2O_5	0.27 ± 0.01	0.4	0.25 ± 0.01	1.8	0.23 ± 0.01	0.4	0.26 ± 0.01	1.9	0.30 ± 0.01	0.9
	K_2O	0.37 ± 0.02	0.6	0.55 ± 0.01	0.2	0.56 ± 0.01	0.5	0.56 ± 0.02	2.8	0.53 ± 0.01	0.5
	CaO	1.0 ± 0.01	0.9	1.4 ± 0.01	0.7	1.5± 0.00	0.3	1.3 ± 0.01	0.9	1.2 ± 0.02	1.9
	TiO_2	6.5 ± 0.1	0.8	9.1 ± 0.1	1.3	7.7 ± 0.1	1.1	9.7 ± 1.3	11.4	4.5 ± 0.2	3.3
	MnO	0.28 ± 0.01	0.7	0.30 ± 0.01	0.7	0.29 ± 0.01	0.5	0.33 ± 0.01	1.7	0.40 ± 0.02	4.3
	Fe_2O_3	17.7 ± 0.04	0.2	16.8 ± 0.04	0.2	17.0 ±0.01	0.3	17.8 ± 0.2	1.0	16.4 ± 0.8	4.5
	CuO	0.04 ± 0.01	1.2	0.03 ± 0.01	2.4	0.04 ± 0.01	1.8	0.04 ± 0.01	2.1	0.03 ± 0.01	4.8
	ZnO	0.02 ± 0.001	2.2	0.02 ± 0.001	1.8	0.02 ± 0.001	1.9	0.04 ± 0.001	5.0	0.02 ± 0.001	2.7
	SrO	0.0096 ± 0.0001	1.0	0.01 ± 0.001	1.9	0.01 ± 0.001	2.9	0.01 ± 0.001	5.2	0.01 ± 0.001	7.6
2ª Sampling campaign	Na_2O	0.19 ± 0.01	3.7	0.19 ± 0.01	5.8	0.20 ± 0.01	3.0	0.29 ± 0.01	1.9	0.20 ± 0.04	1.7
	MgO	0.51 ± 0.02	3.5	0.45 ± 0.01	0.9	0.49 ± 0.02	3.0	0.58 ± 0.01	0.4	0.47 ± 0.01	2.8
	Al_2O_3	16.1 ± 0.2	1.2	13.5 ± 0.1	0.7	13.6 ± 0.2	1.2	12.3 ± 0.1	0.8	14.5 ± 0.2	0.9
	SiO_2	41.8 ± 0.3	0.6	45.3 ± 0.2	0.4	44.1 ± 0.3	0.7	43.3 ± 0.2	0.5	40.8 ± 0.4	1.0
	P_2O_5	0.26 ± 0.01	1.2	0.30 ± 0.01	0.4	0.27 ± 0.01	0.4	0.24 ± 0.01	1.5	0.29 ± 0.01	0.4
	K_2O	0.39 ± 0.01	0.2	0.45 ± 0.01	0.6	0.48 ± 0.01	0.5	0.50 ± 0.01	0.8	0.47 ± 0.01	0.8
	CaO	1.07 ± 0.02	1.4	1.02 ± 0.01	0.5	1.06 ± 0.02	1.7	1.18 ± 0.00	0.3	1.00 ± 0.01	1.1
	TiO_2	6.6 ± 0.1	1.0	6.4 ± 0.1	0.4	6.7 ± 0.2	2.5	12.1 ± 0.5	3.7	5.0 ± 0.1	1.8
	MnO	0.25 ± 0.01	0.9	0.37 ± 0.01	0.9	0.35 ± 0.01	0.6	0.32 ± 0.01	0.4	0.38 ± 0.01	0.2
	Fe_2O_3	18.0 ± 0.1	0.4	17.0 ± 0.2	1.2	17.1 ± 0.1	0.5	17.7 ± 0.1	0.4	17.6 ± 0.1	0.4
	CuO	0.04 ± 0.01	1.2	0.03 ± 0.01	3.7	0.03 ± 0.01	1.8	0.03 ± 0.01	2.6	0.04 ± 0.01	1.4
	ZnO	0.02 ± 0.01	4.5	0.02 ± 0.01	1.5	0.02 ± 0.01	3.2	0.02 ± 0.01	4.3	0.03 ± 0.01	0.8
	SrO	0.01 ± 0.0001	3.2	0.01 ± 0.00001	1.5	0.01 ± 0.0001	0.9	0.00 ± 0.0001	11.4	0.01 ± 0.0001	2.9
3ª Sampling campaign	Na_2O	0.16 ± 0.01	3.3	0.30 ± 0.05	12.8	0.20 ± 0.01	6.1	0.27 ± 0.01	3.9	0.20 ± 0.01	6.3
	MgO	0.46 ± 0.01	0.6	0.70 ± 0.02	2.7	0.49 ± 0.03	6.0	0.53 ± 0.01	2.1	0.50 ± 0.01	0.5
	Al_2O_3	14.0 ± 0.1	0.9	13.9 ± 0.20	1.1	14.0 ± 0.5	1.9	12.2 ± 0.1	1.0	14.6 ± 0.1	0.2
	SiO_2	42.7 ± 0.2	0.4	44.6 ± 0.5	1.1	41.6 ± 0.8	1.6	44.4 ± 0.5	1.0	43.1 ± 0.1	0.1
	P_2O_5	0.24 ± 0.01	0.4	0.25 ± 0.01	1.3	0.27 ± 0.01	2.4	0.25 ± 0.01	0.8	0.29 ± 0.01	1.3
	K_2O	0.37 ± 0.01	0.8	0.60 ± 0.01	0.3	0.47 ± 0.01	0.5	0.55 ± 0.02	3.1	0.49 ± 0.01	0.4
	CaO	1.07 ± 0.01	0.3	1.55 ± 0.02	0.9	1.13 ± 0.02	1.2	1.25 ± 0.01	1.0	1.06 ± 0.01	0.4
	TiO_2	7.00 ± 0.3	3.4	7.85 ± 0.03	0.6	6.50 ± 0.03	0.8	8.50 ± 0.6	11.2	7.00 ± 0.02	0.6
	MnO	0.28 ± 0.01	1.0	0.30 ± 0.01	0.1	0.31 ± 0.01	0.4	0.32 ± 0.01	1.4	0.34 ± 0.01	0.7
	Fe_2O_3	16.6 ± 0.1	0.5	17.0 ± 0.1	0.3	17.0 ± 0.1	0.4	16.9 ± 0.1	0.5	17.4 ± 0.2	0.9
	CuO	0.04 ± 0.01	1.2	0.03 ± 0.01	1.2	0.03 ± 0.01	1.8	0.03 ± 0.01	1.0	0.03 ± 0.01	4.0
	ZnO	0.02 ± 0.01	3.0	0.02 ± 0.01	1.8	0.02 ± 0.01	2.4	0.02 ± 0.01	2.4	0.02 ± 0.01	5.2
	SrO	0.01 ± 0.001	3.3	0.01 ± 0.001	2.0	0.01 ± 0.001	2.9	0.01 ± 0.001	10.3	0.01 ± 0.001	5.2

$\overline{X}$: average concentrations; CI: confidence interval; VC (%): variance coefficient; BF: Barra Funda; RB: Rodeio Bonito; A: Ametista do Sul; IPV: Iraí — Ponte Velha; IBR: Iraí — BR-386.
A total of 45 WD-XRF analyses were performed on the fine fractions of 15 composite sediment samples from the Várzea river.
Source: elaborated by the authors.

Table 5 – Statistical variance analysis by Analysis of Variance (two-tailed, significant $p \geq 0.05$).

Analyte	Variation source	SQ	DF	MQ	F	p value
Na_2O	*Between groups*	0.1	4	0.0	8.9	3.09×10^{-5}
	Within groups	0.1	40	0.0		
	Total	0.1	44	0.0		
MgO	*Between groups*	0.1	4	0.0	3.3	0.02
	Within groups	0.2	40	0.0		
	Total	0.3	44	0.0		
Al_2O_3	*Between groups*	53.8	4	13.4	43.6	4.5×10^{-14}
	Within groups	12.3	40	0.3		
	Total	66.2	44	0.0		
SiO_2	*Between groups*	52.3	4	13.1	15.0	1.45×10^{-7}
	Within groups	34.9	40	0.9		
	Total	87.2	44	0.0		
P_2O_5	*Between groups*	0.0	4	0.0	9.7	1.40×10^{-5}
	Within groups	0.0	40	0.0		
	Total	0.0	44	0.0		
K_2O	*Between groups*	0.1	4	0.0	23.7	4.12×10^{-10}
	Within groups	0.1	40	0.0		
	Total	0.2	44	0.0		
CaO	*Between groups*	0.5	4	0.1	6.2	0.00
	Within groups	0.8	40	0.0		
	Total	1.3	44	0.0		
TiO_2	*Between groups*	101.9	4	25.5	20.1	3.75×10^{-9}
	Within groups	50.6	40	1.3		
	Total	152.5	44	0.0		
MnO	*Between groups*	0.0	4	0.0	23.1	6.09×10^{-10}
	Within groups	0.0	40	0.0		
	Total	0.1	44	0.0		
Fe_2O_3	*Between groups*	2.15	4	0.5	2.5	0.05
	Within groups	8.5	40	0.2		
	Total	10.7	44	0.6		

SQ: sum of squares; DF: degrees of freedom; MQ: mean square; F: Fisher value.
Source: elaborated by the authors.

to the variables (chemical compounds) that contributed to this grouping as shown in the score plots.

The hierarchical cluster analysis generated a dendrogram (Figure 5) similar to the two large clusterings generated by the PCA analysis.

The two different clusters generated by similarity (agglomeration coefficient 0.8) suggest similar geochemical characteristics of these samples. The dendrogram grouped the sediment samples from different sampling campaigns into two clusters, the BF sampling point (upstream the mining zone) and the other sampling points while, by similarity, it grouped the current concentrations of the IPV sampling point (leaving the mining zone).

Determining the environmental geochemical indexes

Table 7 shows the environmental geochemical indices CIA, ER1, and ER2, calculated based on the average concentrations of major oxides. The CIA scores calculated for the Várzea river sediment samples demonstrate extreme chemical weathering, a condition typical of hot and humid regions (GOMES; ALMEIDA; SPERANDIO, 2018; KUSIN *et al.*, 2019).

These results were expected since the matrix analysis characteristics indicated a significant difference between the fluvial sediments and the soil of the watershed due to the heterogeneous mixture of grains caused by the significant transport that weathered particles undergo as a result of the agents such as water (AMOSOVA *et al.*, 2019; SHEN *et al.*, 2018; SILVA *et al.*, 2019).

Moreover, according to the Köppen classification, the study region climate is subtropical with hot summers, without prolonged droughts, and average rainfall distributed throughout the year (SEMA, 2012; SILVA *et al.*, 2019), thus favoring the weathering processes. The scores associated with RE_1 and RE_2 elementary ratios allow identifying the source rock composition (SANG *et al.*, 2018; SOUSA *et al.*, 2018).

Thus, the ER_1 values associated with sediment samples from all sampling points of the Várzea river suggest origin associated with clay minerals. Also, the

Table 6 – Tukey test (two-tailed, significant p 0.05) of major oxides in the sediment samples.

Na_2O	BF	RB	A	IPV	IBR	P_2O_5	BF	RB	A	IPV	IBR
BF		0.0	0.01	0.0	0.1	BF		0.5	1.0	1.0	0.0
RB	6.5		0.7	0.9	0.3	RB	2.3		0.8	0.2	0.0
A	4.8	1.7		0.2	0.9	A	0.8	1.4		0.8	0.0
IPV	7.7	1.2	2.9		0.0	IPV	0.8	3.1	1.6		0.0
IBR	3.7	2.8	1.1	4.0		IBR	7.0	4.8	6.2	7.9	
MgO	BF	RB	A	IPV	IBR	K_2O	BF	RB	A	IPV	IBR
BF		0.0	0.5	0.1	0.7	BF		0.0	0.0	0.0	0.0
RB	4.8		0.4	0.8	0.2	RB	11.7		0.5	1.0	0.3
A	2.3	2.5		0.9	1.0	A	9.4	2.3		0.4	1.0
IPV	3.4	1.4	1.0		0.8	IPV	11.8	0.1	2.4		0.3
IBR	1.7	3.1	0.6	1.7		IBR	8.9	2.8	0.5	2.9	
Al_2O_3	BF	RB	A	IPV	IBR	**CaO**	BF	RB	A	IPV	IBR
BF		0.0	0.0	0.0	0.2	BF		0.0	0.1	0.1	1.0
RB	9.1		1.0	0.0	0.0	RB	5.9		0.4	0.6	0.0
A	9.1	0		0.0	0.0	A	3.5	2.5		1.0	0.2
IPV	17.2	8.0	8.0		0.0	IPV	3.8	2.1	0.4		0.1
IBR	3.1	6.0	6.0	14.1		IBR	0.4	5.5	3.1	3.5	
SiO_2	BF	RB	A	IPV	IBR	TiO_2	BF	RB	A	IPV	IBR
BF		0.0	0.0	0.0	0.8	BF		0.3	1.00	0.0	0.2
RB	9.6		0.0	0.3	0.0	RB	2.9		0.5	0.0	0.0
A	4.0	5.5		0.3	0.4	A	0.7	2.2		0.0	0.1
IPV	6.8	2.7	2.8		0.0	IPV	8.9	6.0	8.2		0.0
IBR	1.6	8.0	2.5	5.2		IBR	3.2	6.1	3.9	12.1	
MnO	BF	RB	A	IPV	IBR	Fe_2O_3	BF	RB	A	IPV	IBR
BF		0.0	0.0	0.0	0.0	BF		0.1	0.3	1.0	0.7
RB	6.5		1.0	1.0	0.0	RB	3.3		1.0	0.1	0.8
A	5.6	0.8		0.8	0.0	A	2.8	0.5		0.2	0.9
IPV	7.2	0.7	1.5		0.0	IPV	0.2	3.5	3.0		0.6
IBR	13.5	7.0	7.9	6.3		IBR	1.8	1.5	1.0	1.9	

BF: Barra Funda; RB: Rodeio Bonito; A: Ametista do Sul; IPV: Iraí — Ponte Velha; IBR: Iraí — BR-386.
Source: elaborated by the authors.

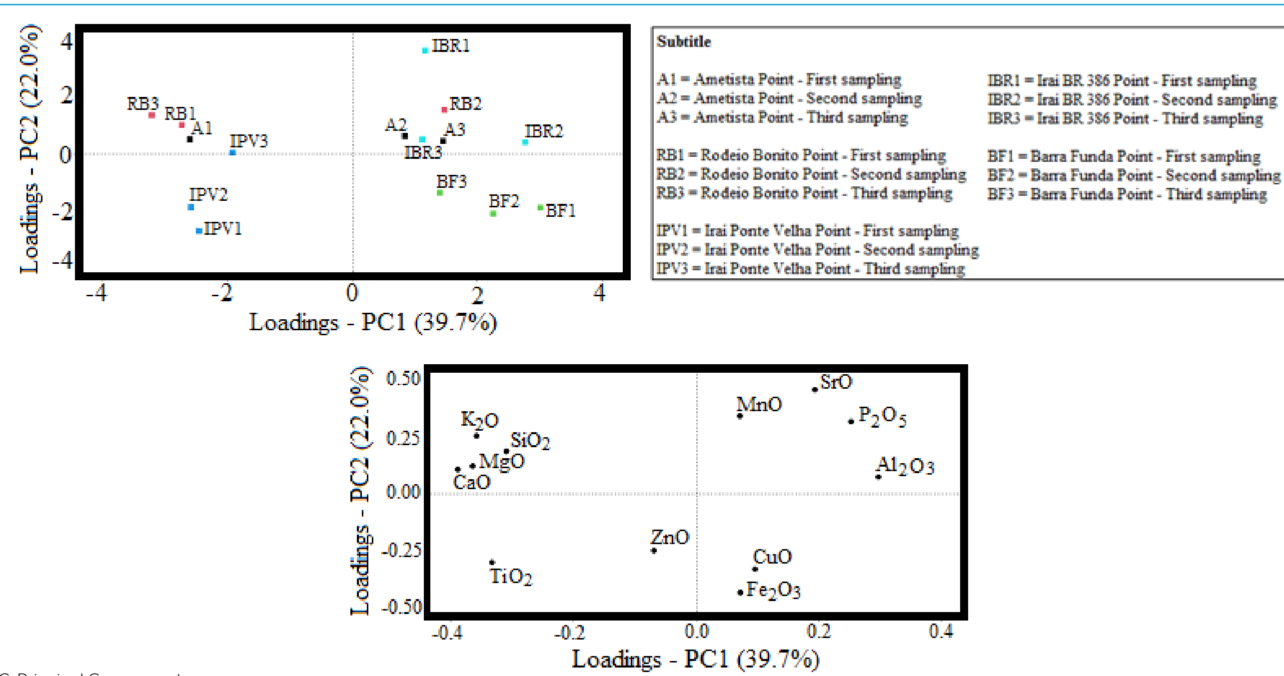

PC: Principal Component.
Source: elaborated by the authors.

Figure 4 – Principal Component Analysis of the average concentrations of major oxides present in sediment samples from the Várzea river, in the state of Rio Grande do Sul.

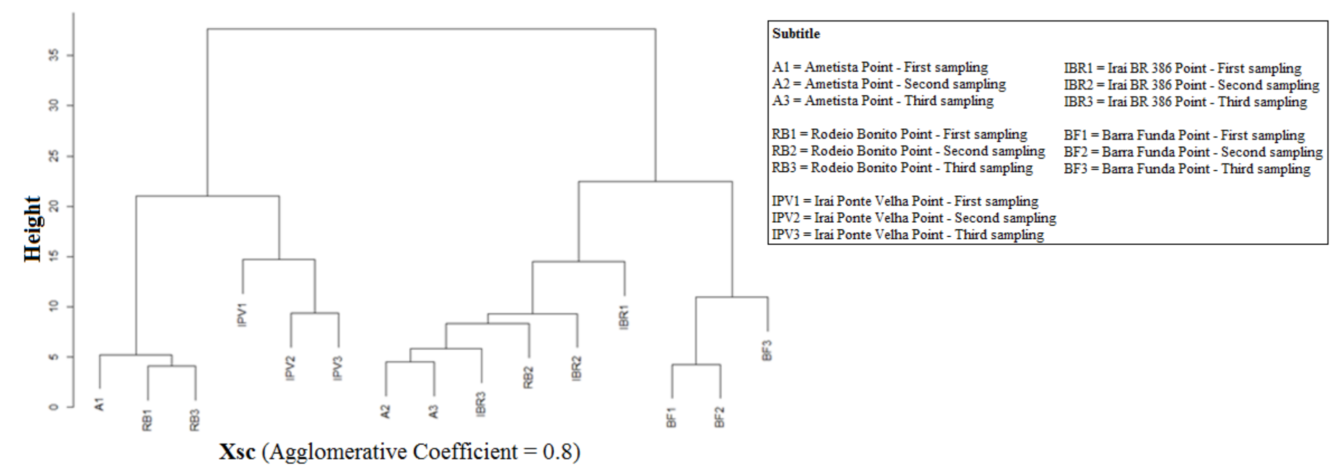

Source: elaborated by the authors.

Figure 5 – Dendrogram resulting from the cluster analysis grouping the average concentrations of major oxides present in sediment samples from the Várzea river, in the state of Rio Grande do Sul .

Table 7 – Environmental geochemical indexes determined for the Várzea river sediments and basalt rocks from tailings in the mining region.

	Chemical Index of Alteration (CIA)	Elementary Ratio (ER_1)	Elementary Ratio (ER_2)
Sediments			
Barra Funda (BF)	90.6	0.03	2.3
Rodeio Bonito (RB)	86.6	0.04	1.8
A (Ametista)	87.5	0.04	2.0
IPV (Iraí – Ponte Velha)	85.6	0.04	1.2
IBR (Iraí – BR-386)	89.2	0.03	2.7
Mining tailings			
Baggio *et al.* (2015)	50.0	0.09	5.7
Hartmann *et al.* (2015)	56.6	0.01	1.2
Korchagin; Caner; Bortoluzzi (2019)	54.2	0.03	4.5

Source: elaborated by the authors.

ER_2 values for sediments from all sampling sites indicate a mafic igneous rock origin such as basalt rocks, for example (GOMES; ALMEIDA; SPERANDIO, 2018; KUSIN *et al.*, 2019; SANG *et al.*, 2018).

The ER_1 and ER_2 values shown in Table 7 suggest an origin associated with clay minerals and mafic igneous rocks, respectively. Likewise, HARTMANN *et al.* (2015) reported similar values for the sediment samples. ER_3 (with values ranging from 2.7 to 3.6) suggests a low compositional maturity of the sediments in the study region. The ER_4 values, ranging between 31.8 and 46.6, indicate the existence of variations in the chemical composition between the sampling points of the Várzea river, in the fine fractions (< 0.063 mm) of the sediment samples. The total content of CaO is different from the other study regions at the Ametista do Sul sampling point (A), mining zone (ARISEKAR *et al.*, 2021; BESSA *et al.*, 2020; SILVA; BATEZELLI; LADEIRA, 2015; ZANARDO *et al.*, 2017). These results are shown in Table 8.

Figure 6 presents the K_2O/Na_2O versus SiO_2 graph that defines the potential geochemical similarity of sediments in the study region, with which is possible to generate a behavioral distinction established through the relationship between the concentrations of major oxides that constitute the fine fractions of the sediment samples.

Table 8 – Environmental geochemical indexes and CaO content determined for the Várzea river sediments and basalt rocks from tailings in the mining region.

	Elementary ratio (ER_3)	Elementary ratio (ER_4)	CaO
Sediments			
Barra Funda (BF)	2.7	46.3	1.0
Rodeio Bonito (RB)	3.3	31.8	1.3
A (Ametista)	3.1	33.8	1.5
IPV (Iraí – Ponte Velha)	3.6	32.5	1.2
IBR (Iraí – BR-386)	2.8	34.5	1.1

Source: elaborated by the authors.

The sampling point of IPV is located immediately after the mineral extraction zone in the municipality of Ametista do Sul, Southern Brazil. The point IPV presents a different behavior, in the graph in Figure 6, from the other sampling points in the water system.

The reference values calculated by the NPI (Table 9) reveal a potential anthropic influence on the water system due to mineral extraction.

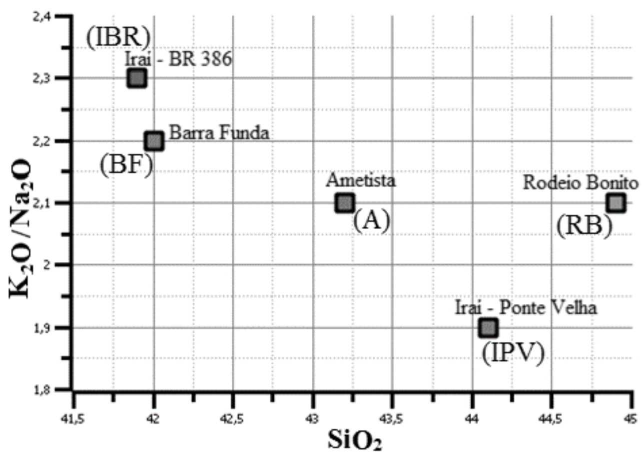

Source: elaborated by the authors.

Figure 6 – Geochemical similarity of sediments sampling points from Várzea river, Southern Brazil.

Table 9 - Nemerow Pollution Index — environmental pollution of sediment samples.

Major oxides	Nemerow Pollution Index				
	BF	RB	A	IPV	IBR
Al_2O_3	1.2	1.0	1.0	0.9	1.0
SiO_2	1.5	1.6	1.6	1.6	1.2
P_2O_5	0.9	1.0	0.9	0.9	1.0
K_2O	1.2	1.7	1.6	1.7	1.2
CaO	1.1	1.5	1.3	1.3	1.1
TiO_2	1.1	1.3	1.1	1.7	1.0
MnO	0.8	1.0	1.0	1.0	1.1
Fe_2O_3	1.1	1.0	1.0	1.1	1.0
CuO	3.0	2.5	2.7	2.9	1.5
ZnO	2.5	2.5	2.4	2.5	1.3

BF: Barra Funda; RB: Rodeio Bonito; A: Ametista do Sul; IPV: Iraí — Ponte Velha; IBR: Iraí — BR-386.
Source: elaborated by the authors.

The baseline (background values) used in this study for the region were determined by Silva *et al.* (2019). The mining tailings around the Várzea river extraction region are basalt rocks with dark tones and are rich in iron, magnesium, titanium, and silica oxides (BAGGIO *et al.*, 2015; KORCHANGIN *et al.*, 2019).

The NPI values can be associated with pluviometric carry processes of the major oxides SiO_2, K_2O, CuO, ZnO present in the sediments embedded mining tailings, indicating the mobility of the content of the basalt rock deposits (ARISEKAR *et al.*, 2021; BESSA *et al.*, 2020). The calculated NPI values show that the Várzea river sediment samples range from polluted for the major oxides CuO and ZnO (point of Iraí BR-386 — IBR), TiO_2 (point of IPV), K_2O (points of IPV, A and Rodeio Bonito — RB) and medium polluted for the major oxides CuO and ZnO (points of Barra Funda — BF, RB, A, and IPV). Furthermore, the NPI values together with the WD-XRF results of the sediment fine fractions from the two sampling campaigns evidence the potential contribution of the SiO_2 major oxides (upstream the BF sampling point that decreases in the downstream sampling points), K_2O, and CaO (in BF, upstream the mining zone, and at the IPV sampling point, in the mining zone) and TiO_2 (IPV, in the mining zone). In Table 9, the differentiation of NPI values for mineral oxide TiO_2, CuO and ZnO at the sampling point (IPV) is highlighted, exiting the mine extraction zone, indicating the pollution of the sediment samples. These concentrations present in sediment samples are often used to identify the provenance and source tectonic environment, as they are relatively immobile during the sedimentary process.

The K_2O is a nutrient that is abundant in the earth's crust and is resistant to weathering processes. Already the CuO is present in range of silicates present in the drainage sediments. In mineral extraction regions, rich in hydrated Fe and Mn oxides, CuO is removed from the drainage sediments by adsorption and recitation in response to changes in pH and Eh. ZnO mobilization is limited during the periods of weathering changes in volcanic rocks and losses due to metamorphism (BAGGIO *et al.*, 2015; BRANCO, 2002; HARTMANN *et al.*, 2015; MINEROPAR, 2001).

Samples of sedimentary rocks and river sediments are usually predominantly characterized by much higher average concentrations of SiO_2 and Al_2O_3 compared to those of K_2O and TiO_2 (BECK *et al.*, 2020; KUSIN *et al.*, 2019; SANG *et al.*, 2018). However, the average concentrations of major oxides determined in the mining zone region of the Várzea river indicate otherwise, thus reinforcing the possibility of anthropic input due to mining activities from semi-precious stones.

CONCLUSIONS

The average concentrations of major oxides such as Al_2O_3, MnO, CaO, SiO_2, K_2O, and TiO_2 present in the fractions of sediment samples from the Várzea river, in Southern Brazil, varied significantly ($p < 0.05$) between the studied sampling points of A, in the mining zone, and IPV, leaving the mining zone. The PCA and the cluster analysis also suggest the existence of three distinct mineral oxide groups, differentiating IPV (leaving the mining zone) and BF (upstream the mining zone) from the other sampling points.

The CIA results indicate extreme chemical weathering of the fluvial sediment samples from the Várzea river. The ER_1 and ER_2 elementary ratios suggest that clay minerals and mafic igneous rocks formed the sediment samples. Also, there is an evident similarity between the ER_2 values of the sediments and those of the basalt rock tailings from the mining zone.

The ER_3 suggests a low compositional maturity, the ER_4 indicate the existence of variations in the chemical composition of the sediments. The content of CaO is different at the sampling point A, mining zone. The K_2O/Na_2O versus SiO_2 graph showed the distinction between the concentrations of major oxides of the sediment samples in IPV.

Regarding, the NPI of the sediments suggests that SiO_2, K_2O, CaO, CuO, ZnO and TiO_2 major oxides occur especially at the IPV sampling point, classifying the sediment samples as from polluted to medium polluted. The results suggest that the environmental stress caused by major oxides supplied to the water system originates from basaltic rock tailings accumulated in front of the mines (sediment formation areas), the byproduct of the mining processes.

ACKNOWLEDGMENTS

The authors thank the support of the Instituto de Pesquisa Hidráulica at Universidade Federal do Rio Grande do Sul (UFRGS), the Universidade Federal de Santa Maria (UFSM), and the grammatical corrections of the manuscript by the journalist Andreia Primaz Eckhardt from O Dois Go Marketing.

AUTHORS' CONTRIBUTIONS

Silva, P.R.B.: Conceptualization, Data curation, Investigation, Methodology, Validation, Writing – original draft. Parizotto, D.: Writing – original draft, Writing – review & editing. Silva, L.R.: Writing – review & editig. Parreira, P.S.: Data curation, Formal analysis. Melquiades, F.L.: Data curation, Formal analysis. Mauad, F.F.: Project administration, Supervision.

REFERENCES

ALVES, W.; FERREIRA, P.; ARAÚJO, M., Challenges and pathways for Brazilian mining sustainability. *Resources Policy*, v. 74, 101648, 2021. https://doi.org/10.1016/j.resourpol.2020.101648.

AMOSOVA, A.A.; CHUBAROV, V.M.; PASHKOVA, G.V.; FINKELSHTEIN, A.L.; BEZRUKOVA, E.V. Wavelength dispersive X-ray fluorescence determination of major oxides in bottom and peat sediments for paleoclimatic studies. *Applied Radiation and Isotopes*, v. 144, p. 118-123, 2019. https://doi.org/10.1016/j.apradiso.2018.11.004

ARISEKAR, U.; SHAKILA, R.J.; SHALINI, R.; SIVARAMAN, B.; JEYASEKARAN, G.; MALINI, N.A.H. Heavy metal concentration in reef-associated surface sediments, Hare Island, Gulf of Mannar Marine Biosphere Reserve (southeast coast of India): The first report on pollution load and biological hazard assessment using geochemical normalization factors and hazard indices. *Marine Pollution Bulletin*, v. 162, 111838, 2021. https://doi.org/10.1016/j.marpolbul.2020.111838

BAGGIO, S.B.; HARTMANN, L.A.; MASSONNE, H.J.; THEVE, T.; ANTUNES, L.M. Silica gossan as a prospective guide for amethyst geode deposits in the Ametista do Sul mining district, Paraná volcanic province, southern Brazil. *Journal of Geochemical Exploration*, v. 159, p. 213-226, 2015. https://doi.org/10.1016/j.gexplo.2015.09.011

BECK, K.K.; MARIANI, M.; FLETCHER, M.S.; SCHNEIDER, L.; AQUINO-LÓPEZ, M.A.; GADD, P.S.; HEIJNIS, H.; SAUNDERS, K.M.; ZAWADZKI, A. The impacts of intensive mining on terrestrial and aquatic ecosystems: A case of sediment pollution and calcium decline in cool temperate Tasmania, Australia. *Environmental Pollution*, v. 265, 114695, 2020. https://doi.org/10.1016/j.envpol.2020.114695

BESSA, A.Z.E.; NGUETCHOUA, G.; JANPOU, A.K.; EL-AMIER, Y.A.; NGUETCHOUA, O.A.N.N.M.; KAYOU, U.R.K.; BISSE, S.B.; MAPUNA, E.C.N.; AMSTRONG-ALTRIN, J.S. Heavy metal contamination and its ecological risks in the beach sediments along the Atlantic Ocean (Limbe coastal fringes, Cameroon). *Earth Systems and Environment*, v. 5, p. 433-444, 2020. https://doi.org/10.1007/s41748-020-00167-5

BILLAH, M.M.; KOKUSHI, E.; UNO, S. Distribution, geochemical speciation, and bioavailable potencies of cadmium, copper, lead, and zinc in sediments from urban coastal environment in Osaka Bay, Japan. *Water, Air, & Soil Pollution*, v. 230, p. 1-13, 2019. https://doi.org/10.1007/s11270-019-4196-8

BRANCO, P.M. *Mapa geológico do estado do Rio Grande do Sul*. Porto Alegre: CRPM Serviço Geológico do Brasil, 2002. 45 p.

BRANDÃO, C.J.; BOTELHO, M.J.C.; SATO, M.I.Z.; LAMPARELLI, M.C. (org.). *Guia nacional da coleta e preservação de amostras*: água, sedimento, comunidades aquáticas e efluentes líquidas. São Paulo: CETESB; Brasília: ANA, 2011.

BURTON, G.A.; JOHNSTON, E. Avaliação de sedimentos contaminados no contexto de Múltiplos Estressores. *Environmental Toxicology and Chemistry*, v. 29, n. 12, p. 2625-2646, 2010.

CROUDACE, I.W.; LÖWEMARK, L.; TJALLINGII, R.; ZOLITSCHKA, B. Current perspectives on the capabilities of high resolution XRF core scanners. *Quaternary International*, v. 514, p. 5-15, 2019. https://doi.org/10.1016/j.quaint.2019.04.002

DIAS, C.H.; CHAVES, M.L.S.C.; JUCHEM, P.L.; ROMANO, A.W. Ocorrências de ametista em basaltos do Triângulo Mineiro (Minas Gerais): descrição e comparações com depósitos similares do Rio Grande do Sul. *Pesquisas em Geociências*, v. 46, n. 3, p. 1-19, 2019. https://doi.org/10.22456/1807-9806.97385

DOTMATICS. *GraphPad Software*: Quick Calcs Outlier Calculator. Dotmatics, 2020. Available at: https://graphpad.com/quickcalcs/Grubbs1.cfm. Accessed on: Jan. 8, 2020.

FUNDAÇÃO ESTADUAL DE PROTEÇÃO AMBIENTAL HENRIQUE LUIS ROESSLER (FEPAM). Bacia hidrográfica do Rio da Várzea. Fepam, 2020. Available at: https://www.fepam.rs.gov.br/qualidade/bacia_uru_varzea.asp. Accessed on: Jan. 8, 2020.

GLOAGUEN, T.V.; MOTTA, P.N.S.D; COUTO, C.F. A grain-size correction for metal pollution indexes in river sediments. *International Journal of Sediment Research*, v. 36, n. 3, p. 362-372, 2021. https://doi.org/10.1016/j.ijsrc.2020.10.005

GOMES, C.H.; ALMEIDA, D.P.M.; SPERANDIO, D.G. Geoquímica de Sedimentos da Confluência das Bacias Hidrográficas Baixo Jacuí e Vacacaí-Mirim, Caçapava do Sul-RS: Implicações para Proveniência e Intemperismo Químico. *Anuário do Instituto de Geociências*, v. 41, n. 3, p. 470-482, 2018. https://doi.org/10.11137/2018_3_470_482

GUILHEN, S.N.; COTRIM, M.E.B.; SAKATA, S.K.; SCAPIN, M.A. Application of the fundamental parameter method to the assessment of major and trace elements in soil and sediments from Osamu Utsumi uranium mine by WDXRF. *REM*: International Engineering Journal, v. 72, n. 4, p. 609-617, 2019. https://doi.org/10.1590/0370-44672018720146

HAMMER, Ø. *Past paleontological statistics*. Version 3.08. Oslo: Natural History Museum University of Oslo, 2015.

HARTMANN, L.A.; MEDEIROS, J.T.N.; BAGGIO, S.B.; ANTUNES, L.M. Controls on prolate and oblate geode geometries in the Veia Alta basalt flow, largest world producer of amethyst, Paraná volcanic province, Brazil. *Ore Geology Reviews*. v. 66, p. 243-251, 2015. https://doi.org/10.1016/j.oregeorev.2014.11.005

HARTMANN, L.A.; PERTILLE, J.; DUARTE, L.C. Giant-geode endowment of tumuli in the Veia Alta flow, Ametista do Sul. *Journal of South American Earth Sciences*, v. 77, p. 51-57, 2017. https://doi.org/10.1016/j.jsames.2017.04.013

HERATH, D.; PITAWALA, A.; GUNATILAKE, J.; IQBAL, M.C.M. Using multiple methods to assess heavy metal pollution in an urban city. *Environmental Monitoring AND Assessment*, v. 190, p. 657-671, 2018. https://doi.org/10.1007/s10661-018-7016-5

INSTITUTO NACIONAL DE METROLOGIA, QUALIDADE E TECNOLOGIA (INMETRO). *Orientação sobre validação de métodos analíticos*: documento de caráter orientativo. DOQ-CGCRE-008. Revisão 5 – Agosto de 2016. Rio de Janeiro: INMETRO, 2018.

KORCHAGIN, J.; CANER, L.; BORTOLUZZI, E.C. Variability of amethyst mining waste: A mineralogical and geochemical approach to evaluate the potential use in agriculture. *Journal of Cleaner Production*, v. 210, p. 749-758, 2019. https://doi.org/10.1016/j.jclepro.2018.11.039

KUSIN, F.M.; AWANG, N.H.C.; HASAN, S.N.M. S.; RAHIM, H.A.A.; AZMIN, N.; JUSOP, S.; KIM, K.W. Geo-ecological evaluation of mineral, major and trace elemental composition in waste rocks, soils and sediments of a gold mining area and potential associated risks. *CATENA*, v. 183, 104229, 2019. https://doi.org/10.1016/j.catena.2019.104229

LONE, A.M.; ACHYUTHAN, H.; SHAH, R.A.; SANGODE, S.J. Environmental magnetism and heavy metal assemblages in lake bottom sediments, Anchar Lake, Srinagar, NW Himalaya, India. *International Journal of Environmental Research*, v. 12, p. 489-502, 2018. https://doi.org/10.1007/s41742-018-0108-9

MINERAIS DO PARANÁ S.A. (MINEROPAR). *Atlas Geoquímico da Folha de Curitiba*. Curitiba: Folha de Curitiba, 2001. 80 p.

MIZAEL, J.O.S.S.; CARDOSO-SILVA, S.; FRASCARELI, D.; POMPÊO, M.L.M.; MOSCHINI-CARLOS, V. Ecosystem history of a tropical reservoir revealed by metals, nutrients and photosynthetic pigments preserved in sediments. *CATENA*, v. 184, 104242, 2020. https://doi.org/10.1016/j.catena.2019.104242

MUSEU DE SOLOS DO RIO GRANDE DO SUL (MSRS). *Solos de Planalto*: unidade de Passo Fundo. 2020. Available at: https://www.ufsm.br/museus/msrs. Accessed on: Jan. 10, 2020.

NEMEROW, N.L. *Stream, Lake, Estuary and Ocean Pollution*. 2 ed. New York: Van Nostrand Reinhold, 1991. 472 p.

OYEDOTUN, T.D.T. X-ray fluorescence (XRF) in the investigation of the composition of earth materials: a review and an overview. *Geology, Ecology and Landscapes*, v. 2, n. 2, p. 1-7, 2018. https://doi.org/10.1080/24749508.2018.1452459

PASTRAN, S.H.; MALLETT, A. Unearthing power: A decolonial analysis of the Samarco mine disaster and the Brazilian mining industry. *The Extractive Industries and Society*, v. 7, n. 2, p. 704-715, 2020. https://doi.org/10.1016/j.exis.2020.03.007

REMOR, M.B.; SAMPAIO, S.C.; RIJK, S.; BOAS, M.A.V.; GOTARDO, J.T.; PINTO, E.T.; SHARDONG, F.A. Sediment geochemistry of the urban Lake Paulo Gorski. *International Journal of Sediment Research*, v. 33, n. 4, p. 406-414, 2018. https://doi.org/10.1016/j.ijsrc.2018.04.009

SANG, P.N.; LIU, Z.; ZHAO, Y.; ZHAO, X.; PHA, P.D.; VAN LONG, H. Chemical weathering in central Vietnam from clay mineralogy and major-element geochemistry of sedimentary rocks and river sediments. *Heliyon*, v. 4, n. 7, e00710, 2018. https://doi.org/10.1016/j.heliyon.2018.e00710

SECRETÁRIA DO AMBIENTE E DO DESENVOLVIMENTO SUSTENTÁVEL (SEMA). *Relatório anual sobre a situação dos recursos hídricos no Estado do Rio Grande do Sul*. Porto Alegre: Governo do Estado do Rio Grande do Sul, 2012.

SANTOS, H.G.; JACOMINE, P.K.T.; ANJOS, L.H.C.; OLIVEIRA, V.A.; LUMBRERAS, J.F.; COELHO, M.R.; ALMEIDA, J.A.; ARAÚJO FILHO, J.C.; OLIVEIRA, J.B.; CUNHA, T.J.F. *Sistema Brasileiro de Classificação de Solos*. 5 ed. rev. e ampl. Brasília: EMBRAPA, 2018. 356 p.

SHEN, M.; GUO, H.; JIA, Y.; CAO, Y.; ZHANG, D. Partitioning and reactivity of iron oxide minerals in aquifer sediments hosting high arsenic groundwater from the Hetao basin, P. R. China. *Applied Geochemistry*, v. 89, p. 190-201, 2018. https://doi.org/10.1016/j.apgeochem.2017.12.008

SILVA, M.L.; BATEZELLI, A.; LADEIRA, F.S.B. Índices de intemperismo e evolução dos paleossolos da Formação Marília, Maastrichtiano da Bacia neocretácea Bauru. *Geochimica Brasiliensis*, v. 29, n. 2, p. 127-138, 2015.

SILVA, P.R.B.; MAKARA, C.N.; MUNARO, A.P.; SCHNITZLER, D.C.; WASTOWSKI, A.D.; POLETO, C. Comparison of the analytical performance of EDXRF and FAAS techniques in the determination of metal species concentrations using protocol 3050B (USEPA). *International Journal of River Basin Management*, v. 14, n.4, p. 401-406, 2016. https://doi.org/10.1080/15715124.2016.1203792

SILVA, P.R.B.; DALLA NORA, F.E.; CASTRO, R.J.; WASTOWSKII, A.D.; MAUAD, F.F. The environmental quality of sediments of rivers near prospection areas of semiprecious rocks. *Environmental Monitoring and Assessment*, v. 191, 364, 2019. https://doi.org/10.1007/s10661-019-7456-6

SOURCEFORGE. *Software de geração gráfica SciDAVis*. 2018. Available at: https://scidavis.sourceforge.net. Accessed on: Jan. 2, 2020.

SOUSA, S.S.C.G.; GUEDES, E.; CASTRO, J.W.A.; ÁVILLA, C.A.; NEUMANN, R. Química Mineral de Granada no Estudo da Proveniência Sedimentar do Litoral Norte do Estado do Rio de Janeiro, Brasil. *Anuário do Instituto de Geociências*, v. 41, n. 2, p. 318-331, 2018. https://doi.org/10.11137/2018_2_318_331

SUNDARARAJAN, S.; KHADANGA, M.K.; KUMAR, J.P.P.J.; RAGHUMARAN, S.; VIJAYA, R.; JENA, B. K. Ecological risk assessment of trace metal accumulation in sediments of Veraval Harbor, Gujarat, Arabian Sea. *Marine Pollution Bulletin*, v. 114, n. 1, p. 592-601, 2017. https://doi.org/10.1016/j.marpolbul.2016.09.016

THE R FOUNDATION. *R - The R Project for Statistical Computing*. [s.d.]. Available at: https://www.r-project.org. Accessed on: March 3, 2022

UNITED STATES ENVIRONMENTAL PROTECTION AGENCY (USEPA) *Framework for ecological risk assessment*. EPA/630/R-92/001. Washington: USEPA, 1992. 58 p.

VOSOOGH, A.; SAEEDI, M.; LAK, R. Heavy metals relationship with water and size-fractionated sediments in rivers using canonical correlation analysis (CCA) case study, rivers of southwestern Caspian Sea. *Environmental Monitoring and Assessment*, v. 188, 603, 2016. https://doi.org/10.1007/s10661-016-5611-x

ZANARDO, A.; NAVARRO, G.R.B.; MONTIBELLER, C.C.; ROCHA, R.R.; MORENO, M.M.T.; DEL ROVERI, C.; AZZI, A.A. Geoquímica e proveniência dos sedimentos da formação Corumbataí na região de Rio Claro/SP. *Geociências*, v. 36, n. 1, p. 30-47, 2017. https://doi.org/10.5016/geociencias.v36i1.12291

ZHAO, X.; HE, B.; WU, H.; ZHENG, G.; MA, X.; LIANG, J.; LI, P.; FAN, Q. A comprehensive investigation of hazardous elements contamination in mining and smelting-impacted soils and sediments. *Ecotoxicology and Environmental Safety*, v. 192, 110320, 2020. https://doi.org/10.1016/j.ecoenv.2020.110320